

Autonomous Chemical Oscillator Circuit Based on Bidirectional Chemical-Microfluidic Coupling

Georgi Paschew, Jörg Schreiter, Andreas Voigt, Cesare Pini, Joseph Páez Chávez, Merle Allerdießen, Uwe Marschner, Stefan Siegmund, René Schüffny, Frank Jülicher, and Andreas Richter*

Autonomous oscillators are a key component of signal processing systems in electronics and biology.^[1,2] The development of oscillators that couple chemical or biological systems with the mechanical domain of microfluidics could stimulate novel concepts for the “smart” handling of fluids and their ingredients. In technology, the realization of chemical oscillators is challenging, in contrast to electronic oscillators. Recently, the construction of microfluidic oscillators has been demonstrated.^[3–7] However, these oscillators operate on purely mechanical principles with no influence of the chemical domain on the fluidic domain. Here we present a microfluidic oscillator circuit employing a chemofluidic volume phase transition transistor for chemical-fluidic coupling and a mixing junction for fluidic-chemical coupling. It operates by constant sources of pressure and flow rate without external control signals and generates oscillations of pressure, flow rate, and chemical concentration. The oscillator is shown to have an oscillation period between 200 and 1000 s, chemical concentrations of alcohol oscillating between 2 wt% and 10 wt%, and flow rates in the range of tens of $\mu\text{L min}^{-1}$.

The mechanical microfluidic oscillators developed by Mosadegh et al.^[3] are relaxation oscillators (akin to astable multivibrators in electronics) based on two field-effect-type valves and two membranes acting as compliances. The oscillators have been used to control subordinate fluid circuits,^[3] to analyze endothelial cell elongation,^[5] and to deliver temporally patterned chemical concentration profiles to living cells.^[4] It was also shown that four independent oscillators on a single chip with periods between 0.4 and 2 h could be operated in parallel, purely driven by gravity.^[5] A different approach for a mechanical microfluidic oscillator based on a simple setup with a single overshooting elastic diaphragm was shown by Xia et al.^[6,7] The device produces fast stable oscillations with a period of about 10 ms with a limited frequency tunability of about 30%. Though frequencies in this range are ideal for rapid flow mixing, they are much too fast compared to many chemical or biological processes. Both microfluidic oscillators discussed can be used to transport reagents, but they are not themselves responsive to chemical concentrations.

G. Paschew, Dr. A. Voigt, M. Allerdießen
Polymeric Microsystems
Institute of Semiconductors and Microsystems
Faculty of Electrical and Computer Engineering
and Center for Advancing Electronics Dresden
Technische Universität Dresden
01062 Dresden, Germany

J. Schreiter, Prof. R. Schüffny
Highly-Parallel VLSI-Systems and Neuromorphic Circuits
Institute of Circuits and Systems
Faculty of Electrical and Computer Engineering
and Center for Advancing Electronics Dresden
Technische Universität Dresden
01062 Dresden, Germany

C. Pini, Prof. A. Richter
Polymeric Microsystems
Institute of Semiconductors and Microsystems
Faculty of Electrical and Computer Engineering
and Center for Advancing Electronics Dresden & Research Training
Group GRK 1865 “Hydrogel-Based Microsystems,”
Technische Universität Dresden
01062 Dresden, Germany
E-mail: Andreas.Richter7@tu-dresden.de

Dr. J. Páez Chávez
Center for Dynamics
Department of Mathematics
Technische Universität Dresden
01062 Dresden, Germany

Dr. J. Páez Chávez
Facultad de Ciencias Naturales y Matemáticas
Escuela Superior Politécnica del Litoral
Km. 30.5 Vía Perimetral
Guayaquil, Ecuador

Dr. U. Marschner
Microsystems Technology
Institute of Semiconductors and Microsystems
Faculty of Electrical and Computer Engineering
Technische Universität Dresden
01062 Dresden, Germany

Prof. S. Siegmund
Center for Dynamics
Department of Mathematics and Center
for Advancing Electronics Dresden
Technische Universität Dresden
01062 Dresden, Germany

Prof. F. Jülicher
Max Planck Institute for the Physics of Complex Systems
01187 Dresden, Germany

Prof. F. Jülicher
Center for Advancing Electronics Dresden
Technische Universität Dresden
01062 Dresden, Germany



DOI: 10.1002/admt.201600005

Chemical oscillations^[8] have been first observed by Belousov and Zhabotinsky in the form of chemical oscillation reactions in the 1950s and are an ongoing topic of scientific investigations.^[9–11] Yoshida et al. showed that it is possible to integrate the Belousov–Zhabotinsky reaction into a pH-sensitive hydrogel with volume phase transition behavior and thus to couple its expansion and contraction to a chemical reaction system that shows pH oscillations.^[12] Incorporating the catalyst covalently into the polymer leads to self-oscillating gels in a nonoscillating chemical environment.^[13–15] It has been suggested to use these gels in a microfluidic setting.^[16] However, their applicability is limited due to the characteristics inherited from the Belousov–Zhabotinsky reaction, such as the harsh media and missing frequency tunability.

The oscillator we present here couples bidirectionally the chemical and the fluidic domain by means of a chemical volume phase transition transistor (CVPT). CVPTs are based on stimuli-responsive hydrogels. Due to their volume phase transition behavior, these materials respond reversibly and reproducibly to small changes of special thermodynamic parameters of the aqueous environment with drastic changes of the volume. Any thermodynamic parameter able to provoke the volume phase transition can be the control signal of the oscillator, especially concentrations of organic solvents, ions, pH value, or the presence of biomolecules.^[17] Here we utilize the hydrogel phase transition stimulated by change of the alcohol concentration in an aqueous solution.

The oscillator employs a microfluidic channel as a delay line for the chemical concentration signal and a CVPT combined with a mixing junction to provide negative feedback. It is interesting to note that nature also uses the approach of a delay and negative feedback in biochemical oscillating systems.^[18] Also in modern electronic systems-on-chip, delay-based oscillators are ubiquitous in the form of ring oscillators in clock generation and frequency synthesis.^[19]

The principle of the oscillator is depicted in **Figure 1**. The circuit is supplied by a constant pressure source (1) with pure water at the buffer channel, a constant flow source (2) with alcohol solution at the mixing point (3), and a constant flow sink (4) at the bypass channel. The fluidic output (6) behind the CVPT with hydrogel (5) is at ambient pressure. Note that in the layout of the oscillator an additional inlet and an additional output branch were added. In the reported experiments they were not used and kept sealed.

We explain the oscillator using the example of 1-propanol as the controlling chemical and an *N*-isopropylacrylamide-sodium-acrylate copolymer as the stimuli-responsive hydrogel. At a fixed temperature, the gel swells in contact with pure water or aqueous solutions with low alcohol concentrations, and it contracts at higher alcohol concentrations. When the hydrogel is swollen, and thus the CVPT closed, the resulting flow rate through the delay line is determined by the sink connected to the bypass channel. The constant flow rate source of the alcohol solution is designed to be a little bit higher than the bypass flow, so that undiluted alcohol solution flows partly through the delay line and partly backward into the buffer line. When the undiluted alcohol solution ($c_{\text{alc}} = 10$ wt%) reaches the hydrogel, the latter begins to shrink, thereby opening the fluidic passage of the transistor and thus allowing for increased

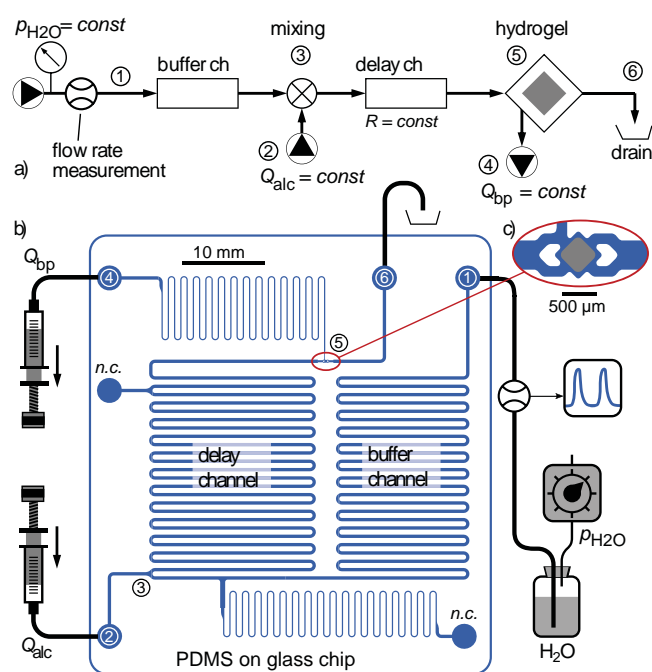


Figure 1. Principle of the oscillator. a) Schematic of the microfluidic circuit. b) Photolithographic layout of the microfluidic chip and schematic laboratory setup. c) CVPT layout detail. Circled numbers in (a) and (b): (1) constant pressure water source, (2) constant flow rate source of aqueous alcohol solution, (3) mixing junction, (4) constant flow rate drain, (5) CVPT, and (6) ambient pressure drain. Unused optional features of the physical chip design are labeled n.c.

flow. Hydrodynamic resistances, the pressure of the water source, and the valve seat geometry are dimensioned such that the increased flow through the now open CVPT is substantially higher than the constant supply of alcohol solution. When the buffer channel has been cleared off the pushed-back alcohol solution, water is added to the alcohol solution at the mixing point (Figure 1b, (3)). While this mixture passes down the delay channel, the diluted solution is homogenized laterally to the channel. Also longitudinal diffusion occurs, however in a range negligible compared to the length of the delay channel. When the diluted alcohol solution reaches the hydrogel, the gel swells again, eventually blocking the valve seat and starting the next cycle of the oscillation.

The oscillator circuit is designed with the help of design automation software for electronic integrated circuits using the analogy of electric and fluidic quantities.^[20–22] In analogy to microelectronics we anticipate that this design automation approach will be a precondition for a transistor based concept of large-scale integrated microfluidic chemical circuits. In the first phase, numerical models of all needed active and passive components are realized (for detailed information, see Supporting Information Section S2). The heart of the oscillator, the CVPT, is modeled by assigning a single size variable to the hydrogel. Depending on the alcohol concentration and the current hydrogel size a rate of size change is applied. The fluidic resistance of the CVPT depends on the width of the two side channels around the hydrogel and is calculated via the Hagen–Poiseuille law for rectangular cross-sections.

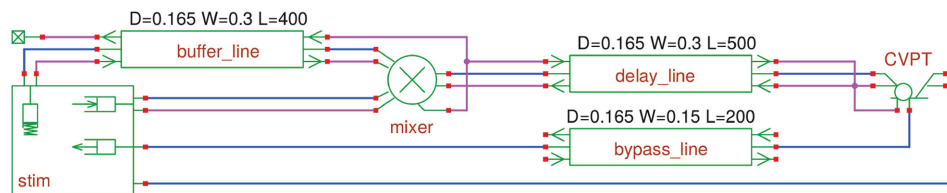


Figure 2. Design with EDA software Virtuoso by Cadence. Schematic representation of the microfluidic circuit and laboratory setup for compact model simulation. Connections drawn in blue represent liquid flow, solute transport with the liquid flow is modeled as connections drawn in purple. Building blocks in green graphics represent instances of compact models. D , W , and L designate the depth, width, and length of a channel in millimeter.

In the second phase, a schematic representation of the microfluidic circuit is generated (Figure 2), comprising connectivity but still neglecting geometry. This facilitates the calculation of all fluidic quantities including their time dependency. As dimensioning of the circuit components and operational parameters of the pumps can be varied easily for repeated simulation, a range of parameters yielding stable oscillation has been determined, and the final optimized dimensioning of the microfluidic channels is chosen to lie well within that range. Once dimensioning is complete, a photomask ready layout is drawn (Figure 1b). The main objectives in this phase are overall size constraints, efficient area utilization, manufacturability, and placement of the inlets and outlets for easy access later in the laboratory.

The operation of the oscillator by means of the CVPT is shown in Figure 3. Videos S1a, S1b, and S1c (Supporting Information) show the chemical-fluidic oscillations in the whole oscillator, the oscillation of the CVPT, and the chemical-fluidic

oscillations at the mixing junction, respectively. The time signal of the oscillator's flow rate in the buffer line (smoothed to eliminate detector noise) is displayed in Figure 4a for the operational parameters $Q_{bp} = 7.56 \mu\text{L min}^{-1}$, $Q_{alc} = 9.8 \mu\text{L min}^{-1}$, and $p_{H_2O} = 88 \text{ mbar}$. By spline interpolation of the maxima and minima the amplitude envelope is determined and used to calculate the long-term signal drift. The power spectrum of the signal (Figure 4b) shows some higher harmonics due to the nonsinusoidal wave form. A comparison measurement is made for a system without hydrogel to determine the system inherent noise, where slow drifts most likely correspond to instabilities of the pumps and the elasticity of the system.

After a fit procedure for the free parameters of the CVPT compact model (see Supporting Information Section S2) a close correspondence of the time signals obtained by simulation (Figure 4c) with experiment was achieved. The bypass output is of special significance since it exhibits a constant flow rate but

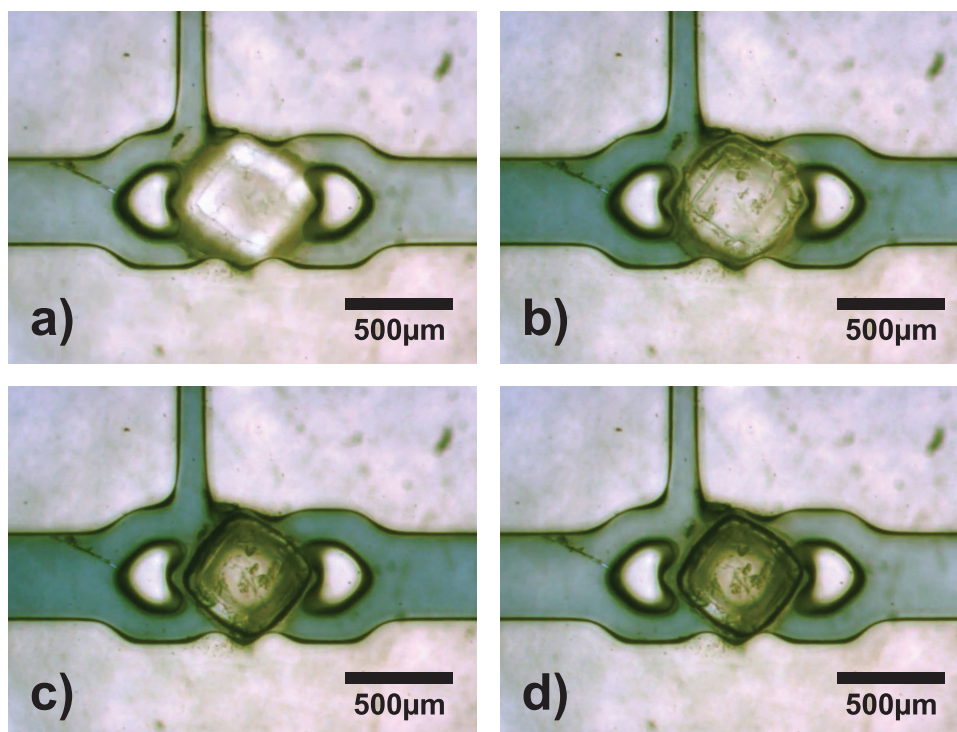


Figure 3. Photographs of the operating CVPT in four different phases. The liquid with high alcohol content is colored by food color. a) Phase 1: valve closed, mostly low alcohol concentration in delay line. b) Phase 2: fluid with high alcohol concentration has reached the hydrogel (valve just beginning to open). c) Phase 3: valve open, mostly fluid with high alcohol concentration in delay line. d) Phase 4: fluid with low alcohol concentration has reached the hydrogel (valve just beginning to close).

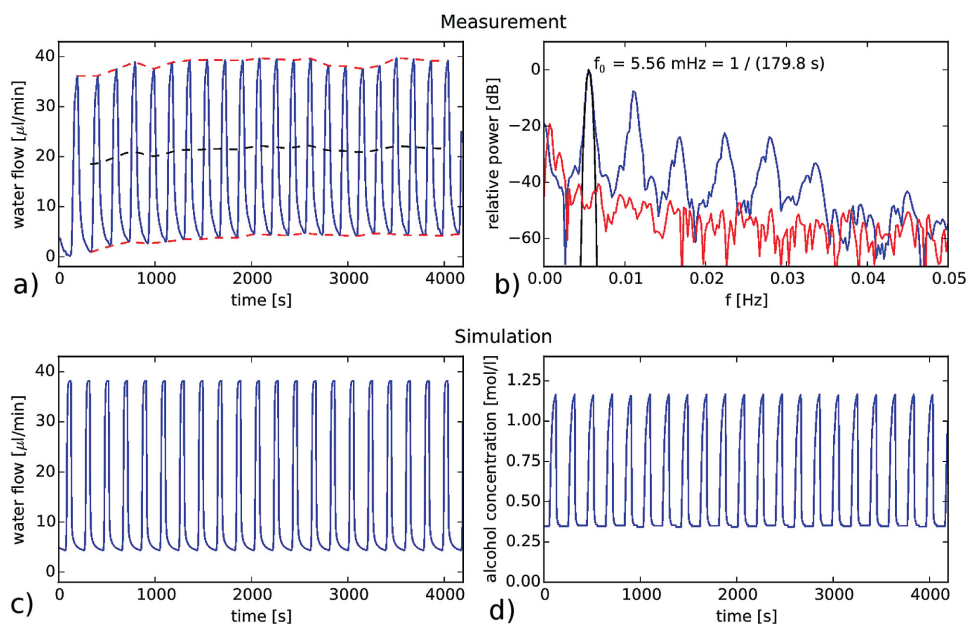


Figure 4. Time signals of the oscillator. a) Time signal of the flow rate at the buffer line (smoothed for the elimination of detector noise). Operational parameters: $Q_{\text{alc}} = 9.8 \mu\text{L min}^{-1}$, $c_{\text{alc}} = 10 \text{ wt}\%$, $Q_{\text{bp}} = 7.56 \mu\text{L min}^{-1}$, $p_{\text{H}_2\text{O}} = 88 \text{ mbar}$. Red graphs show the amplitude envelopes obtained by a spline interpolation. The black dashed line shows the long-term signal drift calculated from the envelopes. b) Power spectrum of the time signal shown in (a) (blue). Spectral line width due to windowing (black). Noise floor obtained from a comparison measurement of the system without hydrogel in the valve (red). c) Simulated signal with the same operation conditions as the experimental signal in (a). d) Simulated signal of the alcohol concentration at the bypass channel.

varying alcohol concentration (Figure 4d) which could be useful for coupling the oscillator to other (e.g., biological) systems.

The stability and the operation range of the oscillator circuit are investigated by varying its operational parameters. As shown in Figure 5a, higher values of flow and pressure sources lead to higher amplitudes and faster oscillations. From the smoothed and drift-corrected signals the periods of each oscillation are determined from the zero-crossings, which allows for the calculation of the period distribution (Figure 5b). For the time signal in Figure 4a the mean period determined by this method amounts to 181.9 s which is close to the inverse of the location of the peak of the first harmonic in the frequency spectrum (Figure 4b). Oscillation periods for given input parameters can be estimated with an accuracy of a factor of about 1.5 by a simplified analytical model which is based on the assumption of a CVPT with an instantaneous reaction time (Supporting Information Section S3).

The operational parameters can be used to tune the oscillation period in a wide range (Figure 5c). Here, the ratio $Q_{\text{alc}}/Q_{\text{pb}}$ is kept at a constant value of 1.25. The existence of oscillatory behavior was predicted by the presence of a Hopf bifurcation in a piecewise-smooth dynamical system modeling the microfluidic oscillator. Figure 5d shows the surface corresponding to the values of the operational parameters Q_{alc} , Q_{pb} , and $p_{\text{H}_2\text{O}}$ for which a Hopf bifurcation occurs, computed via the FORTRAN-based continuation toolbox TC-HAT.^[23] Operational parameters below this surface lead to oscillations while parameters above lead to decaying oscillations, resulting in a steady state of flow rates and alcohol concentrations. We found that the operation of the oscillator is stable for a long time. It is possible to perform daily experiments with the same oscillator

chip containing the same hydrogel for a period of more than three months.

In summary, we have presented a CVPT based oscillator circuit with bidirectional coupling of the chemical with the fluidic domain. In contrast to Belousov–Zhabotinsky-type oscillators the ingredients are nontoxic, the behavior of the oscillator is tunable over a wide range, and the system can be coupled to a wide variety of chemicals. The control signal of an oscillator based on the principles shown here can be any thermodynamic parameter able to provoke a volume phase transition of stimuli-responsive hydrogels within aqueous solutions, for example, pH value or the concentrations of other ions (e.g., of salts), biomolecules like glucose, or organic solvents.^[24–27] The oscillation period can be scaled up or down by the volume of the delay line and the flow rates of the sources, taking into account the reaction time of the CVPT which can be scaled by the choice of hydrogel material and size.

As the PNIPAAm hydrogel is also sensitive toward ethanol,^[28] the current system could be operated to control cells that generate enzymes which are responsible for ethanol production, e.g., yeast cells.^[29] For example, a cell culture chamber could be put into the delay line of the oscillator, where input channel 2 (see Figure 1a) contains the cell growth stimulant glucose instead of alcohol. Depending on the operational parameters the system would either stabilize the cell culture and ethanol production or generate an oscillatory fluctuation of cell population and ethanol production. Another cell species sensitive to ethanol are Golgi cells which could be used in a setup to study the mechanism of alcoholism.^[30] The current oscillator can also be driven with a salt (e.g., NaCl^[25]) instead of alcohol as the active chemical. This widens the applicability in biology where alkali

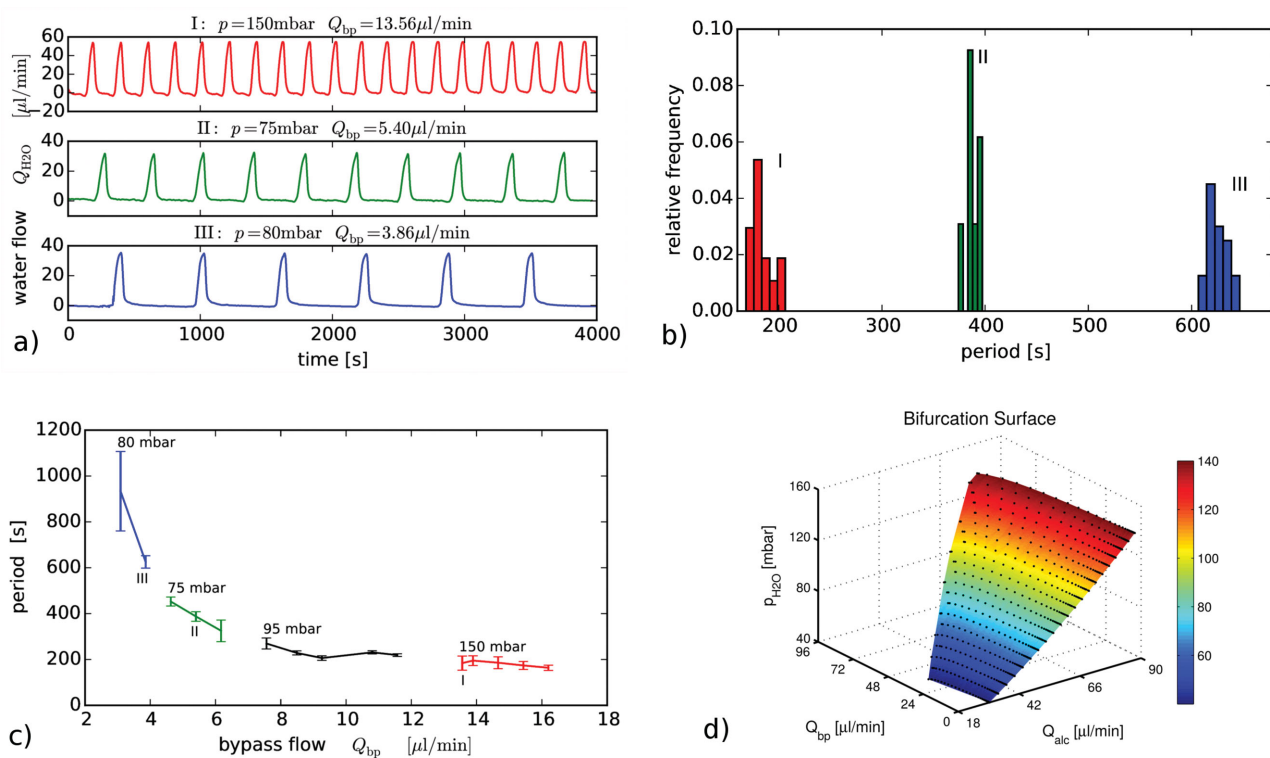


Figure 5. Analysis of the oscillatory behavior. a) Time signals of the flow rate at the buffer line for different operational parameters. b) Period distributions for the time signals shown in (a). c) Mean period as a function of operational parameters. Error bars indicate 3σ . $Q_{\text{alc}}/Q_{\text{bp}} = 1.25$. d) Bifurcation surface obtained from a mathematical model of the chemical oscillator. The points represent the parameter values for which the system undergoes a Hopf bifurcation. For values above the surface the system responds with damped oscillations settling down to a stable equilibrium. Below the surface, this equilibrium becomes unstable and stable periodic behavior appears in the system.

metal and alkaline earth ions are ubiquitous in cell signaling. As chemical oscillations play a fundamental role in cell biology, e.g., in tissue formation, we hope that this will be a future field of application for chemofluidic oscillators in general.

Analogous to microelectronics, we expect that a future trend of microfluidics is the introduction of basic concepts from transistor-based information processing. In digital circuits, three fundamental basic building blocks are logic gates (for data processing), flip-flops (for data storage), and oscillators (to provide timing). We envision microfluidic circuits with the equivalent of these building blocks, based on CVPTs. Chemofluidic oscillators can address a similar range of applications as their microelectronic counterparts: e.g., providing a clock signal for sequential operations, reproducible timing, and synchronization of concurrent processes. Furthermore, the demonstrated tunability is a key factor for synchronization to external references and for calibration in mass production. The simple concept of chemofluidic oscillators with only one active component enables simple integration in larger circuits, e.g., coupled oscillators where effects like phase synchronization and shifts of the oscillation frequency can be utilized. Circuits based on CVPTs can be used to realize hardware defined programs as needed for automated analysis or synthesis with fixed protocols.^[31] On the other hand the bidirectional coupling of the fluidic and the chemical domain allows us to introduce a control layer which enables event controlled programs and

also is the first step toward the goal of flexible programmability within microfluidics.

Experimental Section

Chip Fabrication—Channel Level: For the fabrication of the microfluidic chip a standardized soft-lithographic procedure was used. First, the molding master was realized by structuring a three-layer dry-film-resist, ORDYL SY355 from ELGA EUROPE, on a glass substrate. The polydimethylsiloxane (PDMS) mixture, SYLGARD 184 10A:1B, was then poured over the molding master, degassed at 3 mbar for 60 min, and finally cured in an oven at 60 °C for 40 min.

Synthesis and Structuring of the Hydrogel-Based Component: In a round bottom flask equipped with a magnetic stirrer and a septum *N*-isopropylacrylamide (NiPAAm) and sodium acrylate with a total amount of 1.25 mol was weighted out. The ratio of NiPAAm to sodium acrylate corresponded to 97.5 mol% NiPAAm to 2.5 mol% sodium acrylate. Additionally a portion of the crosslinker 2 mol% *N,N'*-methylene-bisacrylamide was weighted out and filled into the flask. Finally, distilled water was added in order to obtain a polymer solution with a concentration of 1.25 mol L⁻¹. Under constant stirring, the mixture was flushed with argon in the sealed flask for 30 min. Under inert argon atmosphere 2 mol% of the photoinitiator 2-hydroxy-4'-(2-hydroxyethoxy)-2-methylpropiophenone was added to the solution. The solution was then stirred under argon atmosphere for 30 min.

For the fabrication of the active components, a PDMS mould with pits of width 300 $\mu\text{m} \times 300 \mu\text{m}$ and depth 140 μm was prepared. Such a mould is filled with the polymeric solution under inert atmosphere

and sealed with a thin glass slide. Photopolymerization was achieved by exposing the filled and sealed mould to UV-light (mercury short-arc lamp, wavelength of maximum emission 365 nm, power 16 mW cm⁻²) for 20 s at a constant temperature of 5 °C.

Packaging of the Chip: The so-produced active component was manually placed between the holders in the realized PDMS chip. Then the PDMS chip was plasma bonded onto a glass substrate with an exposure time of 2 min at a power of 50 W and an oxygen flow of 40 SSC in the chamber.

Design and Layout Using Electronic Design Automation Tools: Modeling, simulation, and design of the microfluidic circuit was carried out by use of the Design Framework II (DFI) software package of Cadence Design Systems, Inc. Schematic representations of the fluidic systems were generated by use of the tool Virtuoso. A detailed description of the models, simulation, and the design process can be found in Supporting Information Section S2.

Dimensioning of the Components: The width of the hydrogel in the deswollen state amounted to 300 µm; the chamber width was 500 µm. From the compact model simulation the following fabrication parameters were obtained: depth of all channels 0.165 mm, delay and buffer channel width 0.4 mm, delay channel length 500 mm, and buffer channel length 400 mm. In the bypass path a channel was introduced for further experiments. It had negligible influence in the present setup.

Operation of the Microfluidic Circuit: The chip was operated by two syringe pumps and a pressure pump. The pressure pump was operated by de-ionized Millipore water. One syringe pump was operated with a mixture (10 wt%) of propan-1-ol in Millipore water. The second syringe pump acted in backward mode.

Bifurcation Analysis: The bifurcation analysis was performed with the continuation package TC-HAT.^[23] This is a FORTRAN-based toolbox for the numerical continuation and bifurcation detection of periodic orbits of nonsmooth dynamical systems. This package exploits the pseudoarclength numerical continuation applied to boundary-value problems implemented in AUTO 97. TC-HAT, however, does not allow the numerical continuation in two free parameters. Therefore, in order to generate the bifurcation surface, the locus of Hopf bifurcations in the parameter space (Q_{bp} , Q_{alc}) for various fixed values of p_{H2O} was numerically traced.

Supporting Information

Supporting Information is available from the Wiley Online Library or from the author.

Acknowledgements

G.P., J.S., and A.V. contributed equally to this work. G.P. and A.R. had the core idea for the oscillator. G.P., J.S., A.V., and U.M. further developed the concept. J.S. performed the simulation, design, and layout under supervision of R.S. with additional help from A.V. for device modeling. The simplified analytic model of the oscillator was developed by A.V. J.P.C. developed a dynamical system model of the oscillator and carried out its bifurcation analysis under supervision of S.S. The working design of the CVPT was experimentally developed by M.A. C.P. manufactured the microfluidic circuit and characterized the dynamic behavior of the oscillator with support from G.P. G.P. and C.P. took the videos. The main text was written by A.V. with support from J.S., C.P., A.R., and F.J. F.J. provided crucial input regarding oscillator characterization, data evaluation, and modeling. The whole project was supervised by A.R. This work was supported in part by the German Research Foundation (DFG) within the Cluster of Excellence "Center for Advancing Electronics Dresden" (cfaed). Additional funding was provided by the German Research Foundation (RI1294/7, GRK1865

"Hydrogel-based Microsystems") and the European Social Fund. J.P.C. was supported by a Georg Forster Research Fellowship granted by the Alexander von Humboldt Foundation, Germany.

Received: January 15, 2016

Published online: February 24, 2016

- [1] R. K. Garg, A. Dixit, P. Yadav, *Basic Electronics*, Laxmi Publications, New Delhi, India, **2008**.
- [2] K. Kruse, F. Jülicher, *Curr. Opin. Cell Biol.* **2005**, *17*, 20.
- [3] B. Mosadegh, C.-H. Kuo, Y.-C. Tung, Y. Torisawa, T. Bersano-Begey, H. Tavana, S. Takayama, *Nat. Phys.* **2010**, *6*, 433.
- [4] S.-J. Kim, R. Yokokawa, S. C. Leshner-Perez, S. Takayama, *Anal. Chem.* **2012**, *84*, 1152.
- [5] S.-J. Kim, R. Yokokawa, S. Cai Leshner-Perez, S. Takayama, *Nat. Commun.* **2015**, *6*, 7301.
- [6] H. M. Xia, Z. P. Wang, W. Fan, A. Wijaya, W. Wang, Z. F. Wang, *Lab. Chip* **2011**, *12*, 60.
- [7] H. M. Xia, Z. P. Wang, V. B. Nguyen, S. H. Ng, W. Wang, F. Y. Leong, D. V. Le, *Appl. Phys. Lett.* **2014**, *104*, 024101.
- [8] A. T. Winfree, *J. Chem. Educ.* **1984**, *61*, 661.
- [9] S. A. Giannos, S. M. Dinh, B. Berner, *Macromol. Rapid Commun.* **1995**, *16*, 527.
- [10] M. Iranifam, M. A. Segundo, J. L. M. Santos, J. L. F. C. Lima, M. H. Sorouraddin, *Luminescence* **2010**, *25*, 409.
- [11] M. Orbán, K. Kurin-Csörgei, I. R. Epstein, *Acc. Chem. Res.* **2015**, *48*, 593.
- [12] R. Yoshida, H. Ichijo, T. Hakuta, T. Yamaguchi, *Macromol. Rapid Commun.* **1995**, *16*, 305.
- [13] R. Yoshida, T. Takahashi, T. Yamaguchi, H. Ichijo, *J. Am. Chem. Soc.* **1996**, *118*, 5134.
- [14] Y. Zhang, N. Zhou, N. Li, M. Sun, D. Kim, S. Fraden, I. R. Epstein, B. Xu, *J. Am. Chem. Soc.* **2014**, *136*, 7341.
- [15] T. Masuda, A. Terasaki, A. M. Akimoto, K. Nagase, T. Okano, R. Yoshida, *RSC Adv.* **2014**, *5*, 5781.
- [16] D. Suzuki, T. Kobayashi, R. Yoshida, T. Hirai, *Soft Matter* **2012**, *8*, 11447.
- [17] A. Richter, in *Hydrogel Sensors and Actuators* (Eds: G. Gerlach, K.-F. Arndt), Springer, Berlin **2009**, pp. 221–248.
- [18] B. Novák, J. J. Tyson, *Nat. Rev. Mol. Cell Biol.* **2008**, *9*, 981.
- [19] J. Jalil, M. Bin Ibne Reaz, M. A. M. Ali, *IEEE Microwave Mag.* **2013**, *14*, 97.
- [20] K. W. Oh, K. Lee, B. Ahn, E. P. Furlani, *Lab Chip* **2012**, *12*, 515.
- [21] S.-S. Li, C.-M. Cheng, *Lab Chip* **2013**, *13*, 3782.
- [22] F. A. Perdignes, A. Luque, J. M. Quero, *IEEE Ind. Electron. Mag.* **2014**, *8*, 6.
- [23] P. Thota, H. Dankowicz, *SIAM J. Appl. Dyn. Syst.* **2008**, *7*, 1283.
- [24] D. J. Beebe, J. S. Moore, J. M. Bauer, Q. Yu, R. H. Liu, C. Devadoss, B.-H. Jo, *Nature* **2000**, *404*, 588.
- [25] A. Richter, A. Türke, A. Pich, *Adv. Mater.* **2007**, *19*, 1109.
- [26] K.-F. Arndt, D. Kuckling, A. Richter, *Polym. Adv. Technol.* **2000**, *11*, 496.
- [27] A. Baldi, Y. Gu, P. E. Loftness, R. A. Siegel, B. Ziaie, *J. Microelectromechanical Syst.* **2003**, *12*, 613.
- [28] A. Richter, J. Wenzel, K. Kretschmer, *Sens. Actuators B Chem.* **2007**, *125*, 569.
- [29] L. Wang, X.-Q. Zhao, C. Xue, F.-W. Bai, *Biotechnol. Biofuels* **2013**, *6*, 133.
- [30] J.-J. Huang, C.-T. Yen, M.-L. Tsai, C. F. Valenzuela, C. Huang, *Alcohol. Clin. Exp. Res.* **2012**, *36*, 2110.
- [31] R. Greiner, M. Allerdisen, A. Voigt, A. Richter, *Lab Chip* **2012**, *12*, 5034.